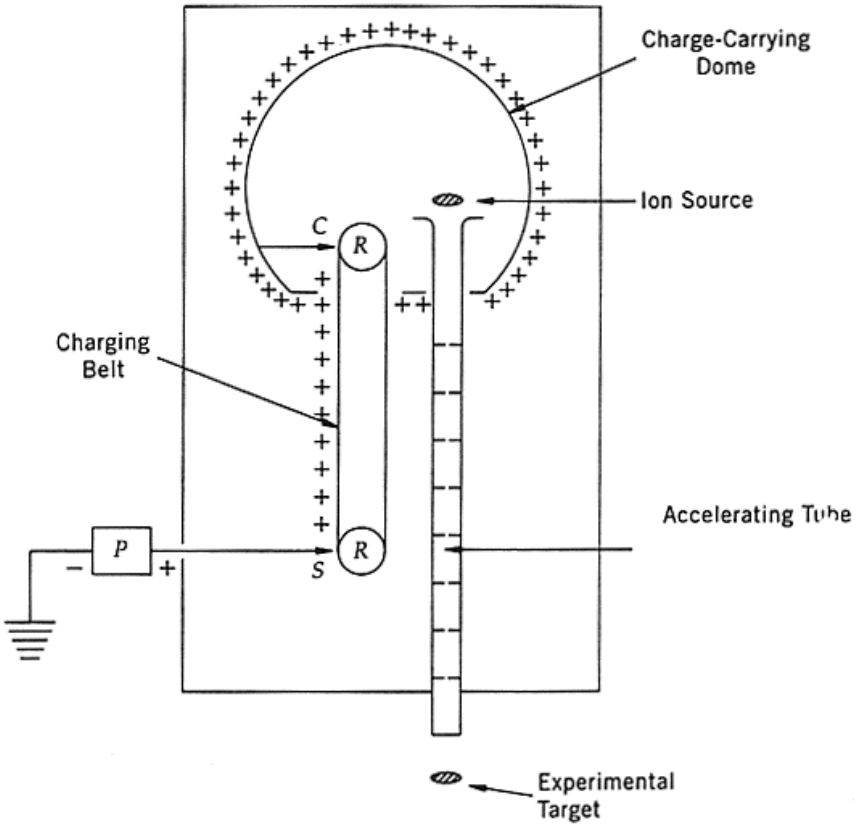

Fig.4.1 The principle of the Van de Graaff accelerator

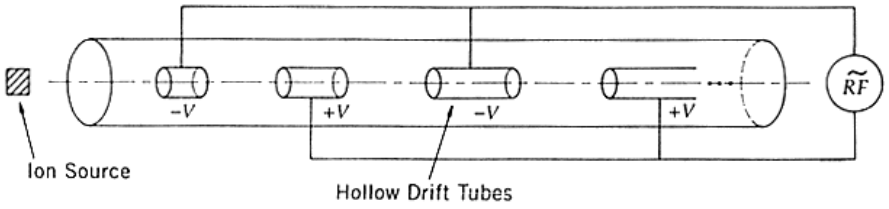

Fig.4.2 Acceleration in a linear accelerator

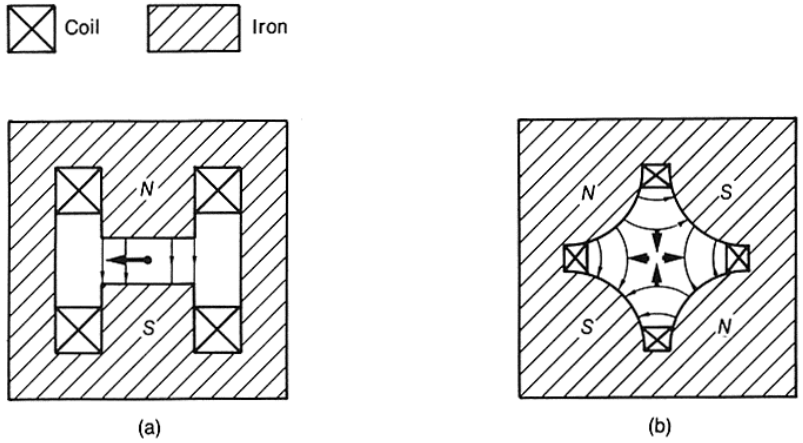

Fig.4.3 Cross-section of (a) typical bending (dipole) magnet and (b) focusing quadrupole) magnet. The light arrows indicate field directions; the heavy arrows, the force on a positive particle travelling into the paper.

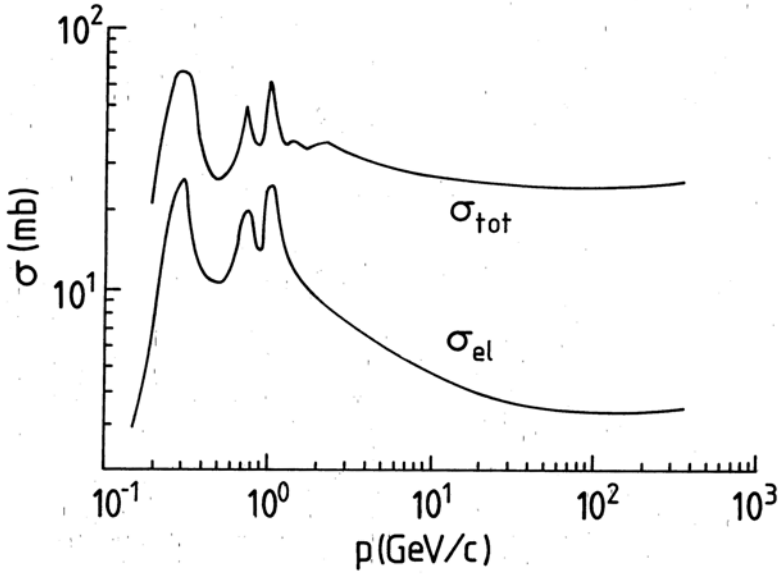

Fig.4.4 Total and elastic cross-sections for $\pi^- p$ scattering as a function of the pion laboratory momentum

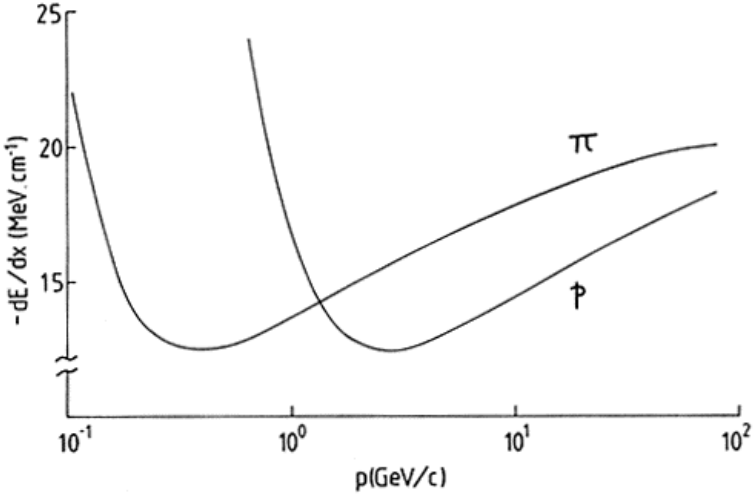

Fig.4.5 Ionization energy loss for charged pions and protons in lead

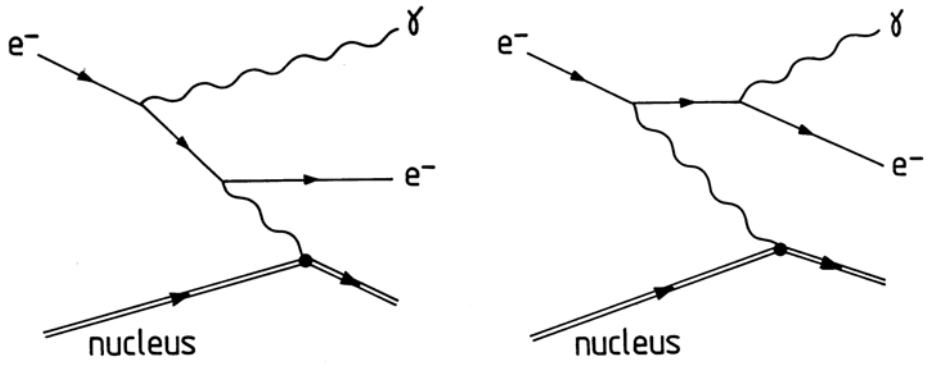

Fig.4.6 Dominant Feynman diagrams for the bremsstrahlung process $e^- + (Z,A) \rightarrow e^- + \gamma + (Z,A)$

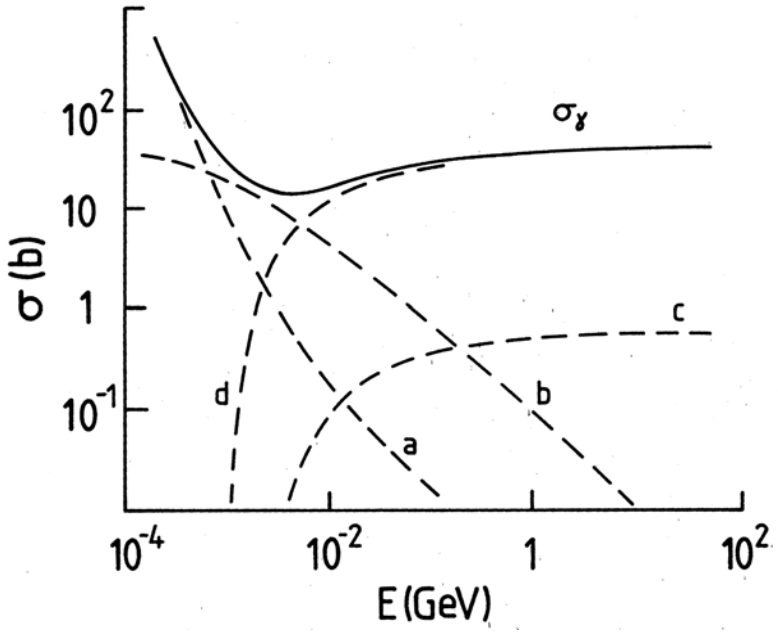

Fig.4.7 Total photon cross-section σ_γ on a lead atom, together with the contributions from (a) the photoelectric effect, (b) Compton scattering, (c) pair production in the field of the atomic electrons, and (d) pair production in the field of the nucleus.

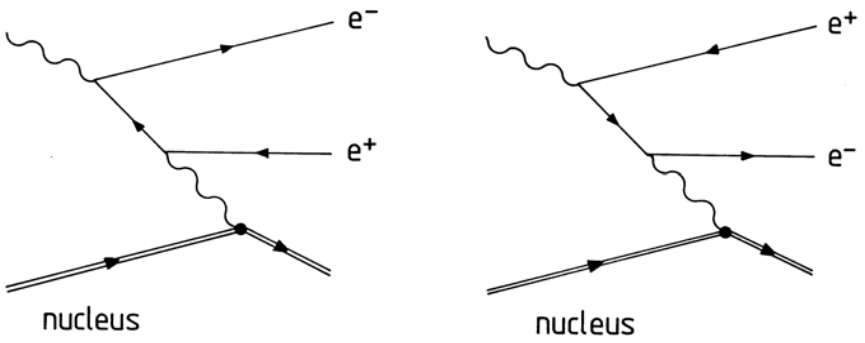

Fig.4.8 The pair production process $\gamma + (Z,A) \rightarrow e^- + e^+ + (Z,A)$

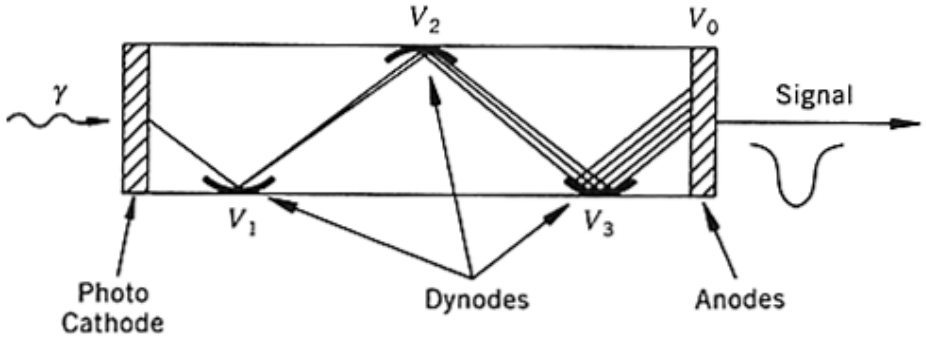

Fig.4.9 Schematic diagram of the main elements of a photomultiplier tube

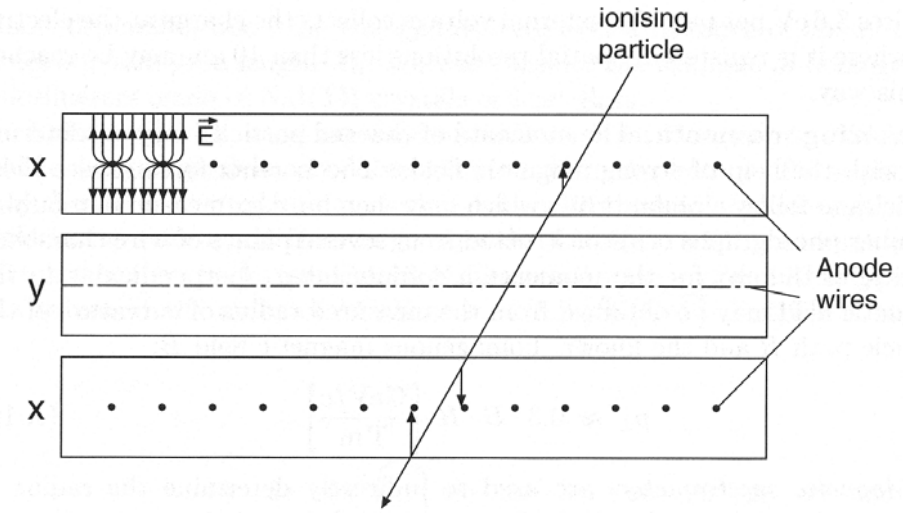

Fig.4.10 A group of three proportional chambers. The anode wires of the x-layers point into the page; those of the y-layers run at right angles. The cathodes are the edges of the chambers. A positive voltage applied to the anode wires generates a field as shown in the upper corner. A particle crossing the chamber ionizes the gas and the electrons drift along the field lines to the anode wires. In this example, there would signals from one wire in the upper x-plane and two in the lower x-plane.

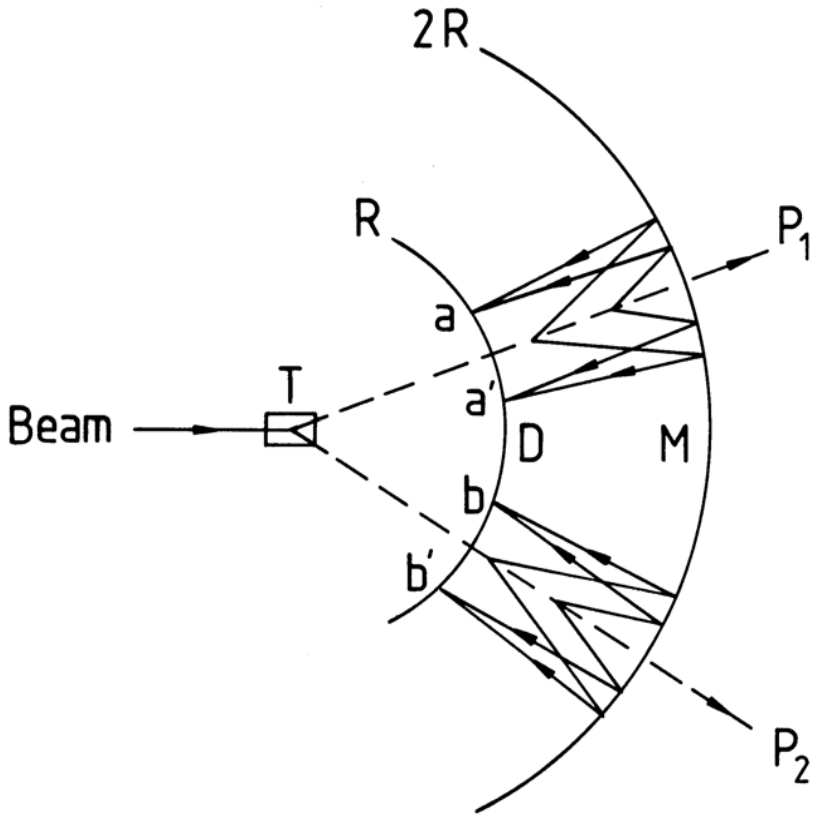

Fig.4.11 Two particles P_1 and P_2, emitted from the target T, emit Čerenkov radiation on traversing a medium contained between two spheres of radius R and 2R. The mirror M on the outer sphere focuses the radiation into ring images at aa′ and bb′ on the inner detector sphere D. The radii of the ring images depend on the angle of emission of the Čerenkov radiation and hence on the velocities of the particles.

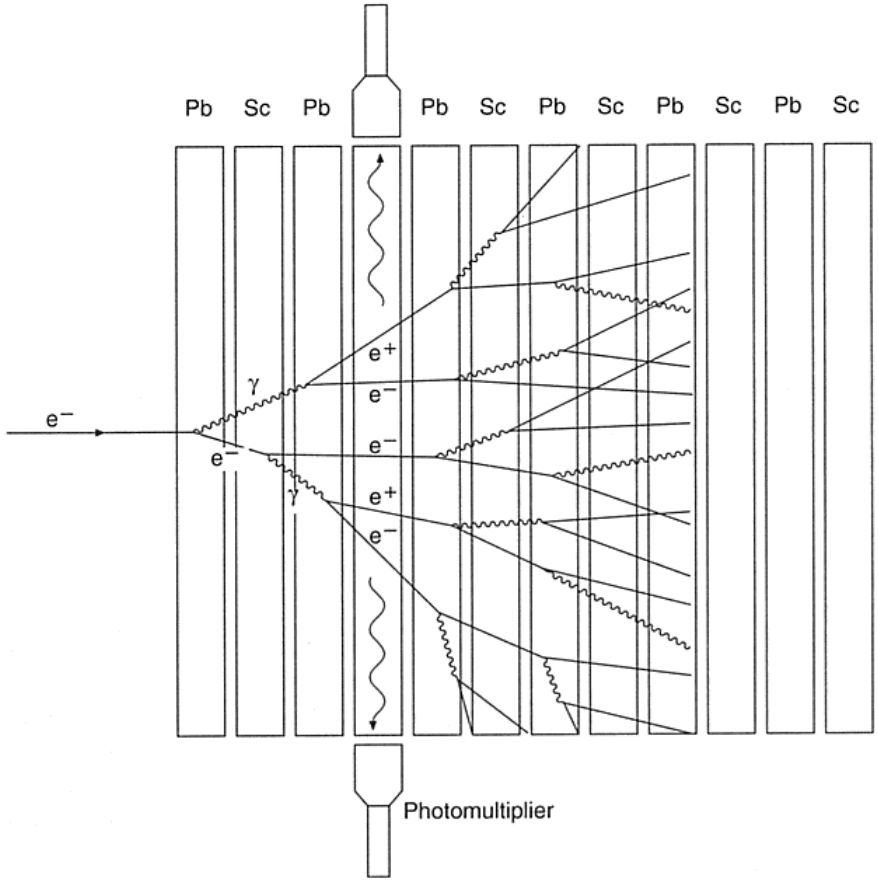

Fig.4.12 Electromagnetic shower development inside a sampling calorimeter. (The particle tracks are not continued to the rear of the detector.)

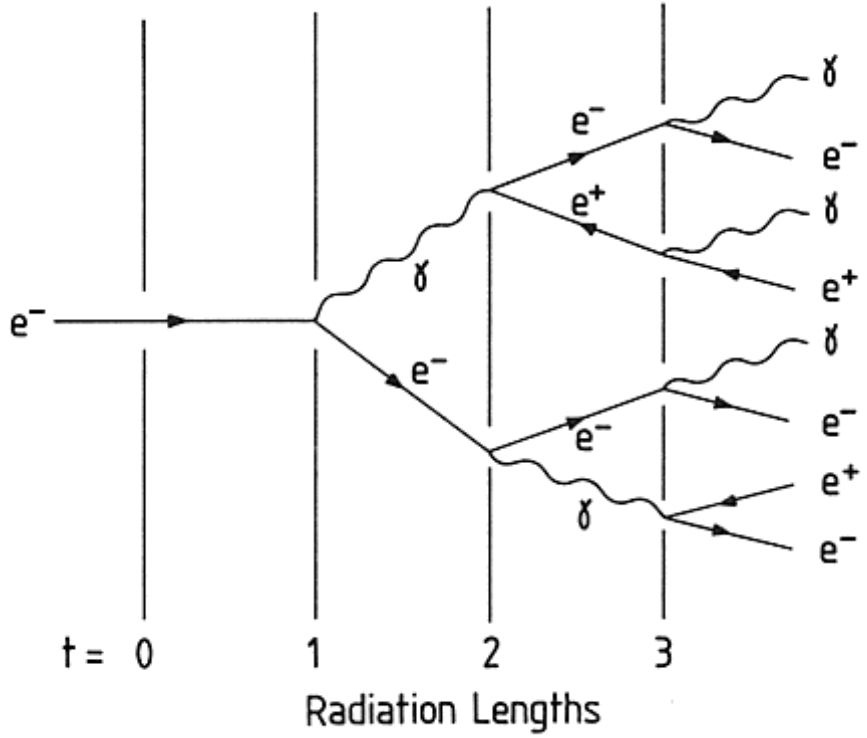

Fig.4.13 Simple model for the development of an electromagnetic shower

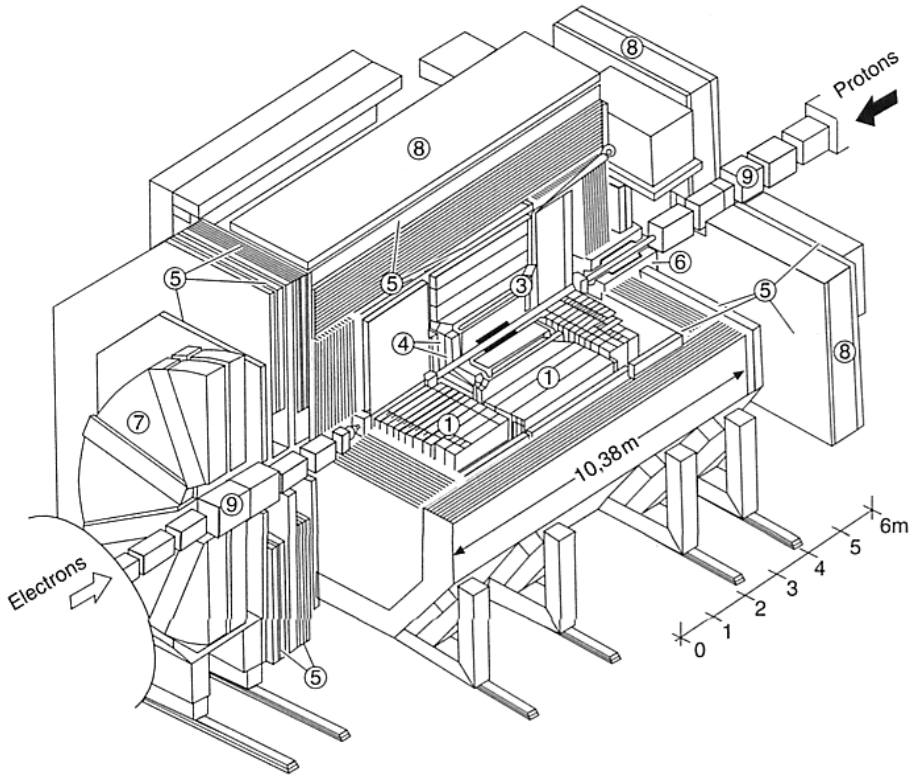

Fig.4.14 The ZEUS detector at the HERA collider at DESY, Hamburg